Stanford Exploration Project, Report 129, May 6, 2007, pages 213–232

Improving multiple prediction in image space using ADCIGs for limited-offset recordings

Madhav Vyas

ABSTRACT

Auto-convolution is a convenient way of generating multiple models and is the basis for Surface Related Multiple Prediction (SRMP). The completeness of the multiple model, however, relies on recording all the primary paths that contribute to multiple generation. In practice, with limited offset recordings and in areas of complex subsurface geometries (especially steep dips), we might record only the multiple path and not the primary, leading to incomplete multiple models. In image space, this translates to modeling multiples at fewer opening angles than are actually present. In this article, I show that the Angle Domain Common Image Gathers (ADCIGs) of multiple models provide useful angular information which may be used to infill or extrapolate missing angles and account for the missing multiples in the model generated using SRMP.

INTRODUCTION

Removing multiples from seismic data is essential to producing interpretable subsurface images. Multiples can be categorized on the basis of kinematics and the mechanism of generation. Multiples can be of different types, including specularly reflected or diffracted multiples, peg-leg multiples, surface-related multiples or inter-bed multiples. Strong surface related multiples associated with the free surface are common in marine surveys. With the increase in marine acquisition, surface-related multiples have received more attention, and techniques for handling and removing these multiples have improved.

Kinematics of surface-related multiples can be predicted by auto-convolution of recorded data (Anstey and Newman, 1966). However, due to discrepancies between modeled and observed multiples in terms of their amplitudes and frequency content, direct subtraction is not possible. Various iterative and adaptive subtraction schemes have been proposed in the past to address this issue. The problem of multiple removal can also be attacked in image space instead of in the data domain (Sava and Guitton, 2003, 2005; Alvarez et al., 2004). There are some intuitive reasons to prefer image-space prediction over data-space modeling. First, the image space is much smaller than the data space, and hence there are associated computational savings. Second, if we assume perfect knowledge of the velocity, discriminating between multiples and primaries with the help of common-image-point gathers (offset and angle) is fairly straightforward.

Artman and Matson (2006) extended the SRMP approach through commutability of wavefield extrapolation and convolution to predict multiples in image space during shot-profile migration. The image-space SRMP algorithm is computationally cheaper than first carrying out SRMP in the data space and then migrating the data and the multiple model independently to the image space. However, since SRMP is based on convolving recorded data with itself, it yields perfect multiple prediction only when we record all the primary paths that lead to multiple generation. This is true when either our recording geometry is infinite or the subsurface structure is flat. In practice, neither of the aforesaid conditions are likely; in addition, there are situations when the primary escapes the recording geometry, but the corresponding multiple, after hitting a steeply dipping reflector bounces back in and gets recorded. Figure 1 shows the ray path for one such possibility. It is not possible to predict this multiple using SRMP, because we do not record the contributing primaries.

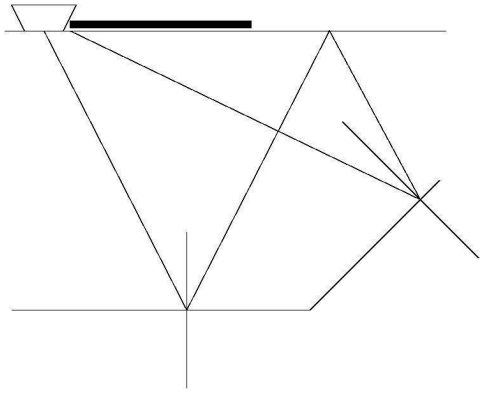

Figure 1: A ray path illustrating the situation where the primary escapes the recording geometry but the multiple bounces back and gets recorded. madhav1-raypath [NR]

It is difficult to model such multiples; however, image space gives us a better chance to handle them. We can make use of the redundancy present in the image space to address this problem. Multiple events in the data space migrate to a single point in image space (if perfect multiple velocity) but with different opening angles, and a missing event in data space translates to a missing angle in image space. If we can spread the information consistently from one opening angle to another, we may be able to reconstruct the missing part of the multiple model. When the migration velocity is perfect, events in the image space will appear flat in the angle domain, and we can easily infill the missing angles to reconstruct the multiple model. But in general, multiples have very different velocities than the primaries recorded at similar times and show curvature in the angle domain when migrated with the true velocity. The task of infilling is thus not as straightforward as it is for flat gathers. There are two ways to approach this: either we can migrate with the multiple velocity, do infilling and then demigrate, or alternatively, we can use Radon-style transforms to infill gathers with curvature.

In this article I first demonstrate the problem using a simple synthetic example and then illustrate a possible corrective approach. I give a second example using the Sigsbee model, which is a more realistic case.

THEORY - SRMP

A multiple event can be modeled or predicted by convolution of two primary traces. Only surface-related multiples (multiples that reflect at the surface) can be estimated by such a prediction scheme. Understanding the assumption of convolving raw traces with themselves rather than with the primaries, multiple prediction (SRMP) can be written in the Fourier domain (Berkhout and Verschuur, 1997) as

$$M(\mathbf{x}_g;\mathbf{x}_s,\omega) = \sum_{\mathbf{x}_a} R(\mathbf{x}_g;\mathbf{x}_a,\omega)R(\mathbf{x}_a;\mathbf{x}_s,\omega)\,, \tag{1}$$

where R is the data-space volume of shot-gathers defined at geophone (x_g) and source (x_s) locations on the acquisition surface. M is the multiple model and ω is the frequency. Equation 1 is a trace-by-trace operation to produce the multiple prediction with any geophone-source combination. Artman and Matson (2006) showed that equation 1 can be re-written in terms of wavefields ($U(\mathbf{x},\mathbf{x}_s)$) as

$$M_{z=0}(\mathbf{x};\mathbf{x}_s,\omega) = \sum_{\mathbf{x}_a} U_{z=0}(\mathbf{x};\mathbf{x}_a,\omega)U_{z=0}(\mathbf{x}_a;\mathbf{x}_s,\omega)\,. \tag{2}$$

With a little bit of algebra and the use of reciprocity, Artman and Matson (2006) also showed that equation 2 reduces to

$$m_z(\mathbf{x},\mathbf{h}) = \sum_{\mathbf{x}_s}\sum_{\omega} U_z(\mathbf{x}+\mathbf{h};\mathbf{x}_s,\omega)U_z(\mathbf{x}-\mathbf{h};\mathbf{x}_s,\omega)\,, \tag{3}$$

where m_z is the multiple model in image space defined at the image coordinates, surface location x and offset h. A direct analogy can be drawn between equation 3 and the imaging condition for shot-profile migration, the difference being that the shot wavefield is now replaced by the receiver wavefield.

Using the scheme proposed above, multiple prediction can be carried out in the image space, which is theoretically equivalent to doing SRMP in the data space, followed by migration. In this article, I use both the image-space SRMP and data-space SRMP to generate multiple models.

SYNTHETIC DATA

I generate a synthetic data set using finite-difference modeling for the velocity model given in Figure 2. The velocity model is a combination of a flat layer and a layer having a dip of 30 degrees. The simulation is done with a free surface condition to model multiple events as well. I modeled about 225 shots with offsets ranging from -8000 ft to 8000 ft and shot spacing of 40 ft. Figure 3 is a sample shot record corresponding to a shot located at a surface location of 5000 ft. In the given shot record we have primaries and both first- and second-order multiples coming from the flat as well as the dipping reflector. There are also different types of first-order multiples having varied trajectories, including multiple bounces on the flat layer,

multiple bounces on the dipping layer and one bounce each on the flat and dipping layers. Finally, there are second-order multiple events which have higher degrees of freedom in terms of possible ray combinations and have further complicated trajectories. Most of the multiple analysis carried out henceforth focuses on first order multiples.

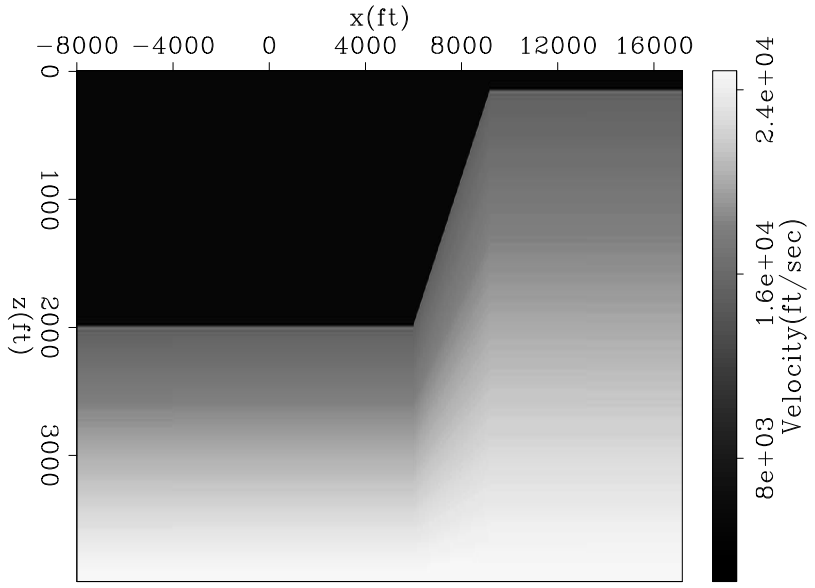

Figure 2: Velocity model used for modeling the synthetic data madhav1-vel.dip1 [ER]

First Order Multiples - Analytics

To identify different multiples and to understand their behavior, I analytically modeled the ray paths for all possible first-order multiple events for the given synthetic model. For simplicity of referencing to these events I use the nomenclature given in Table 1.

Table 1. Nomenclature for different first order multiples.

Type	Ray-path	Name
1	Both the bounces on the flat part	FF
2	First bounce on the flat part and second on the dipping	FD
3	First bounce on the dipping part and second on the flat	DF
4	Both the bounces on the dipping part	DD

Equations 4 and 5 give the travel time and offset as a function of θ (take-off angle) for the event FF,

$$t(\theta) = \frac{4d}{V\cos\theta}, \tag{4}$$

$$h(\theta) = 4d\tan\theta. \tag{5}$$

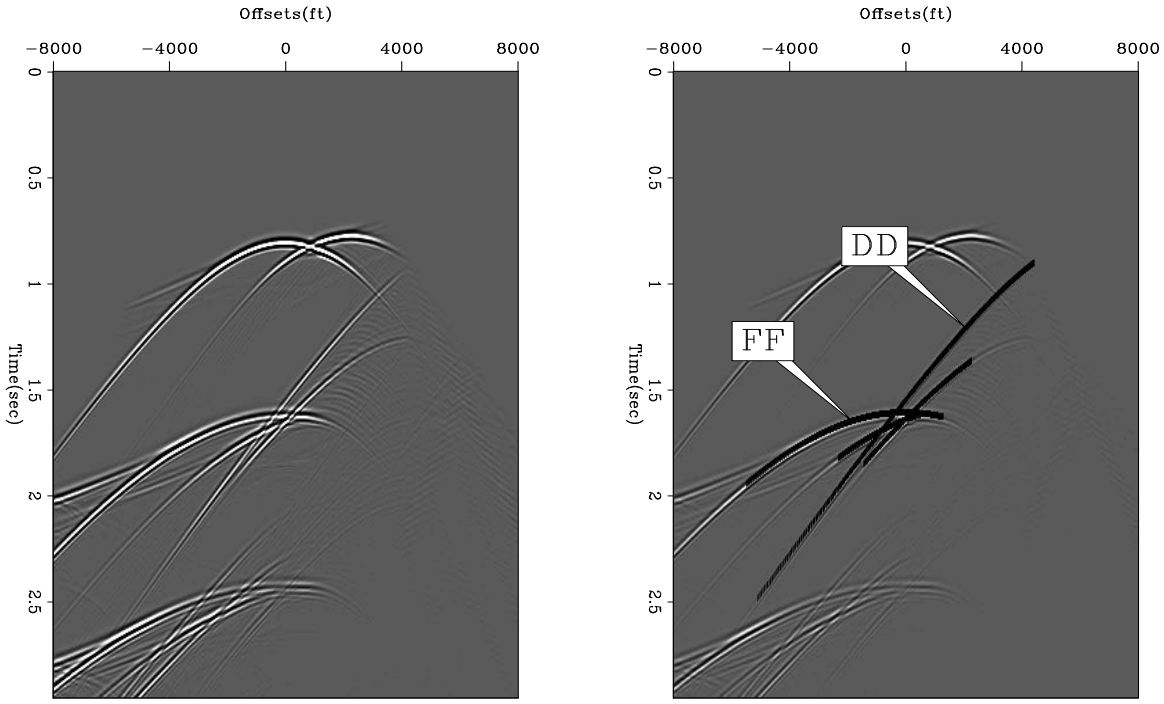

Figure 3: (a) A shot record corresponding to a shot located at a surface location of 5000. (b) Shot record with first order multiples modeled analytically overlaid on them madhav1-shot5000 [CR]

In the equations above, d is the depth of the flat reflector, V is the velocity, and h and t are offset and travel time respectively. There are different conditions and constraints on the value of θ depending on the shot location, which determines the range of take-off angles where these events take place and get recorded. Equations 6 and 7 give the expressions for travel time and offsets for the event FD.

$$t(\theta) = \frac{1}{V}.\{\frac{2d}{\cos\theta} + \frac{(x_d + \frac{d}{\tan\alpha} - x_s - 2d\tan\theta)(\sin\alpha)}{\cos(\alpha-\theta)}.[1 + \frac{\cos\theta}{\cos(2\alpha-\theta)}]\} \tag{6}$$

$$h(\theta) = [\sin\theta - \cos\theta\tan(2\alpha-\theta)].\frac{\sin\alpha}{\cos(\alpha-\theta)}.[x_d + \frac{d}{\tan\alpha} - x_s - 2d\tan\theta] + 2d\tan\theta \tag{7}$$

In these equations, x_d is the horizontal location where the dipping reflector meets the flat layer, x_s is the source location and α is the dip of the dipping reflector. There are two other possibilities for the first-order multiples: DF and DD. Travel time and offsets are given in equations 8 and 9 for the first category and equations 10 and 11 for the second category.

$$t(\theta) = \frac{1}{V}\{(x_d + \frac{d}{\tan\alpha} - x_s)\frac{\sin\alpha}{\cos(\theta-\alpha)}[1 + \frac{\cos\theta}{\cos(2\alpha-\theta)}] + \frac{2d}{\cos(2\alpha-\theta)}\} \tag{8}$$

$$h(\theta) = (x_d + \frac{d}{\tan\alpha} - x_s).\frac{\sin\alpha}{\cos(\theta-\alpha)}.\{\sin\theta - \cos\theta\tan(2\alpha-\theta)) - 2d\tan(2\alpha-\theta\} \tag{9}$$

$$t(\theta) = \frac{1}{V}.[x_d + \frac{d}{\tan\alpha} - x_s].\frac{\sin\alpha}{\cos(\theta-\alpha)} \times$$
$$\times [1 + \frac{\cos\theta}{\cos(2\alpha-\theta)} + \frac{\cos\theta}{\cos(2\alpha-\theta)}.\frac{\cos(\theta-\alpha)}{\cos(3\alpha-\theta)} + \frac{\cos\theta}{\cos(4\alpha-\theta)}.\frac{\cos(\theta-\alpha)}{\cos(3\alpha-\theta)}] \quad (10)$$

$$h(\theta) = [x_d + \frac{d}{\tan\alpha} - x_s].\frac{\sin\alpha}{\cos(\theta-\alpha)}.[\sin\theta$$
$$- \cos\theta\tan(2\alpha-\theta) - \frac{\cos\theta.\cos(\theta-\alpha)}{\cos(3\alpha-\theta)}.\{\tan(2\alpha-\theta)+\tan(4\alpha-\theta)\}] \quad (11)$$

Once again, all the above equations are functions of the parameter θ and are valid only for a range of θ values corresponding to angles at which the event actually takes place. On Figure 3 (b) are overlaid the first-order multiple events modeled using the above equations.

Surface Related Multiple Prediction

The next step is to model these multiples using SRMP. Ideally, when we record all the offsets, SRMP could perfectly model surface-related multiples. In this section I test how the SRMP algorithm performs when we do not have access to far offsets. To simulate this situation, I throw away half the modeled offsets, keeping only the offsets from -4000 ft to 4000 ft instead of -8000 ft to 8000 ft. We would expect SRMP to fail for events that bounce back into the recording geometry (Figure 1). For the given synthetic example, first-order multiples that have either one or both bounces on the dipping surface bounce back into the recording geometry (FD,DF,DD). In the subsequent analysis we focus on the multiple which gets back into the recording geometry after bouncing twice on the dipping surface (DD), though the same may apply to other kinds of multiple events as well.

To estimate first-order multiples using SRMP, we need to record two primary paths that contribute to the multiple. In Figure 4, I draw a crossplot corresponding to a shot at a surface location of 5000 ft. Where on X axis is the offset at which the multiple DD is actually recorded, and on Y axis is the offset of both the primaries contributing to this multiple. Note that for the multiple recorded at an offset of about -4000 ft, the corresponding primaries are recorded at offsets of -5800 ft and -1800 ft. When we limit the maximum recording offset to -4000 ft, we will not be able to model this multiple event as one of the primary events will not be recorded. Likewise, any multiple event having either of its primaries recorded at offsets greater than 4000 ft will not be modeled. The circled portion in the figure indicates that the multiples recorded at offsets between -4000 ft and -2000 ft will not be modeled as one of the contributing primaries come at an offset greater than the maximum recording offset (4000 ft). The maximum recording offset would thus limit us to be only able to model multiples recorded at offsets of -2000 ft or less.

Figure 5 shows the shot gather, the multiple model created using SRMP, and the gather after adaptively subtracting the multiple model. Notice that the tail of the particular multiple event DD is not modeled between offsets of -2000 ft to -4000 ft (circled), as predicted by the crossplot in Figure 4.

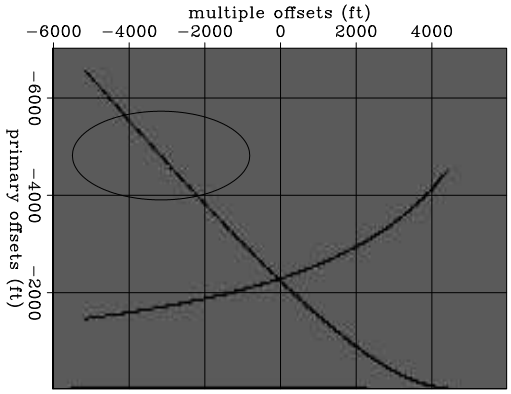

Figure 4: Crossplot between offsets of recorded multiples and primaries contributing to those multiples madhav1-offsets [NR]

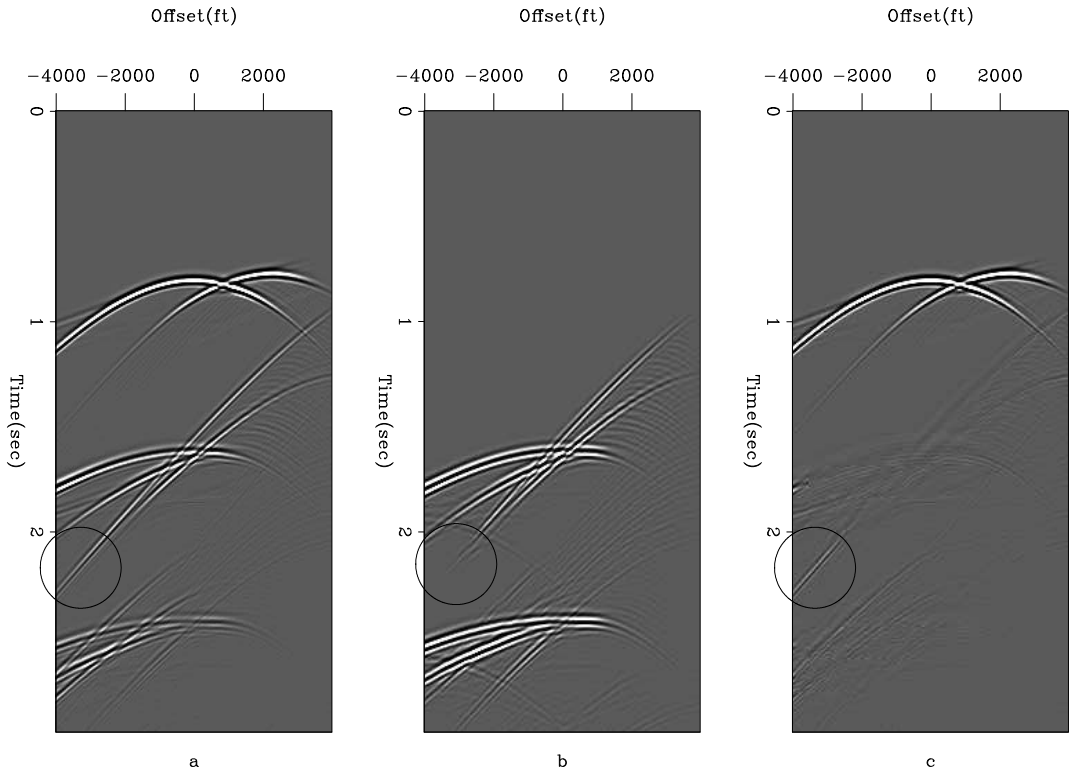

Figure 5: The (a) shot gather, (b) the multiple model and (c) the gather after subtracting the multiple model madhav1-srme.so.5000 [CR]

Once we migrate the data after subtracting the multiple model obtained using SRMP, we expect to see some remains of the multiples in the image space, since we were unable to completely model all the multiple events. Figure 6 compares the two images obtained by migrations carried out on the data with and without multiple subtraction. The image obtained from the data after removing the multiple model is devoid of the flat portion of the first-order multiple, but some portion corresponding to the dipping layer remains. This dipping multiple in the image space corresponds to the event DD in data space; we were not able to model this perfectly because of limited-offset recording. Some multiple energy also remains in the bottom portion of the image, corresponding to the second-order multiple energy, but here I limit the analysis to the first-order multiple events.

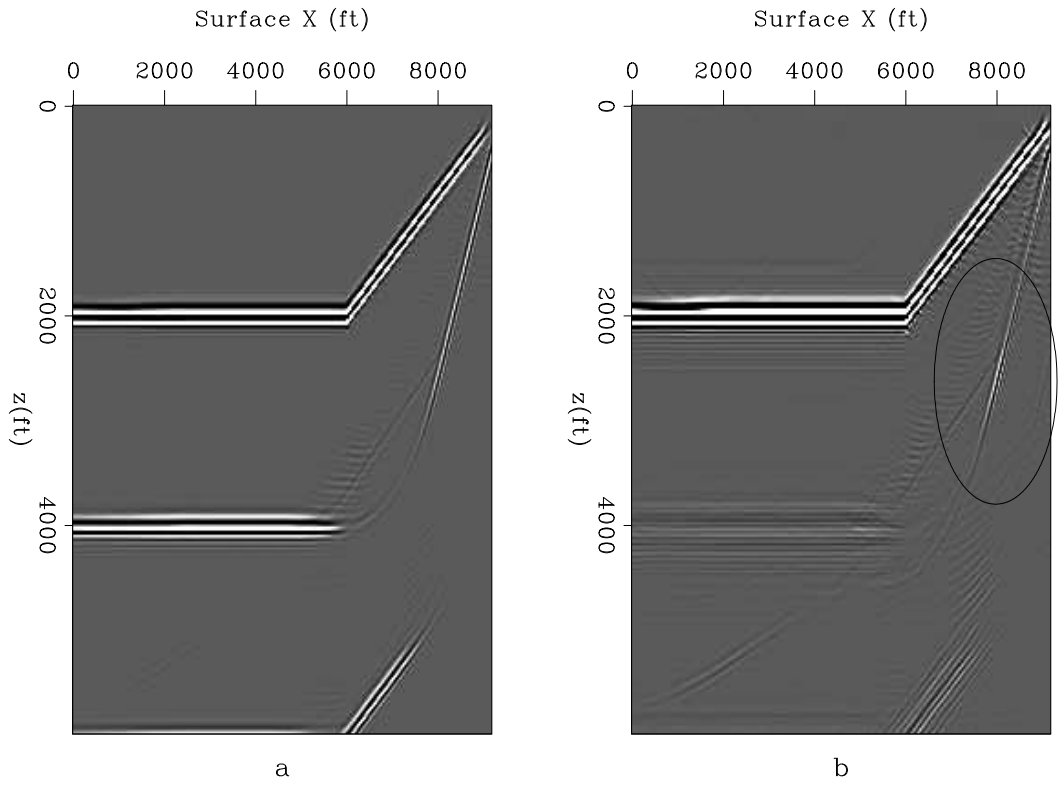

Figure 6: Image obtained by migrating the data (a) before multiple removal and (b) after multiple removal madhav1-compim [CR]

Use of ADCIGs

There are many events in data space that migrate to the same point in image space (if the migration velocity is perfect), but with different opening angles. In the class of events discussed above, because of limited recording geometries we do not expect to model all those angles. However, if we can capture some subset of angles, we can make use of the ADCIGs to infill these missing angles and generate a more complete multiple model. When migration velocity is same as the multiple velocity, this reduces to simple interpolation or extrapolation, because

events will be perfectly flat in the ADCIGs. In cases of imperfect velocity, Radon-style transforms can be used to accomplish the same goal.

To illustrate the point, I extract an ADCIG corresponding to a surface location of 8000 ft (where the dipping multiple persists). Figure 7 (a) is the ADCIG of the recorded data and shows angles at which the multiple is actually illuminated. Figure 7 (b) displays the illumination range of the modeled multiple. Note that the modeled multiple is missing at far angles where the recorded multiple exists. This indicates that SRMP in this case was unable to model far angles. Figure 7 (c) is the ADCIG for the data obtained after removing the multiple model generated using SRMP (data space removal). Again, we were able to get rid of multiple energy close to zero offset, but we still have multiple energy at far offsets.

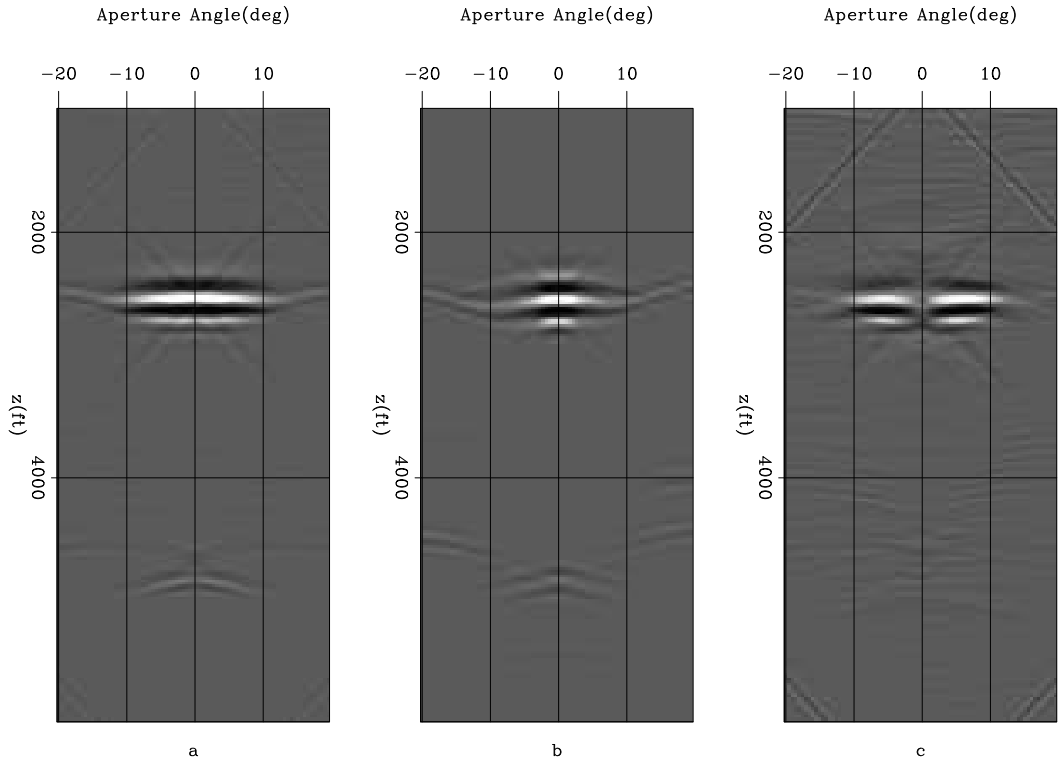

Figure 7: ADCIGs for (a) complete data (b) multiple model and (c) data after removing the multiple model madhav1-ADCIG [CR]

For a given velocity model and recording geometry, we can analytically compute the angles up to which we will be able to model a particular multiple, and the angles up to which it will be actually recorded. The multiple event DD maps as a dipping reflector with twice the dip in image space. ADCIGs above also show the angular illumination for this multiple event. Figure 8 shows a plot between illumination angle and offsets for an image point located at the multiple event, with twice the dip of the original and having an X position of 8000 ft. The plot shows the relation between surface offsets and illumination angles for the first-order multiple event DD along with the two primaries that contribute towards it. It can be noticed from the plot that if we limit our recording from -4000 ft to 4000 ft, the multiple will be illuminated from -10 to +10 degrees. To model this multiple we need to record both the primaries that

contribute towards it. The plot shows that for limited offsets we record both primaries only in an angular range of -5 to +5 degrees. This would be the range in which we will be able to model the multiple, which reiterates the inability of SRMP to model multiples at far opening angles, with such geometries and limited offsets.

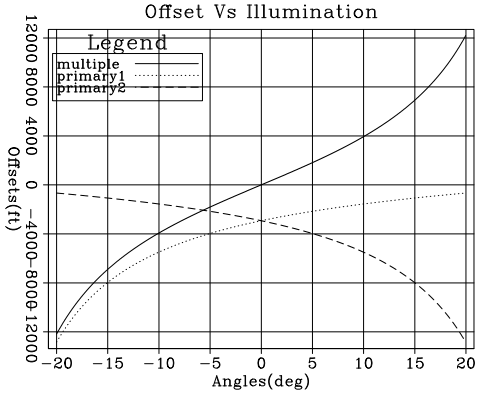

Figure 8: The relation between recording offsets and opening angles for the multiple event with several bounces on the dipping layer, and the primaries that contribute to it, for an image point corresponding to the X position of 8000 ft. madhav1-angoff [NR]

To obtain Figure 7 (c) we constructed the multiple model in the data space, removed it from the data and then migrated it to image space and constructed ADCIGs. Equivalently, this process could have been carried out in image space, in which case we would migrate the data and the multiple model independently to the image space and then do the subtraction.

Reconstructing missing angles

The advantage of working with image-space SRMP is that we have access to angle-domain information, which can be used to infill the missing angles in the multiple model. When using the perfect migration velocity, angle gathers look flat and extrapolating farther angles is fairly straightforward. A simplistic approach like stacking along angles and then spraying the normalized energy to other angles (stack and spray) can work well in case of flat gathers.

I use the algorithm proposed by Alvarez and Guitton (2006) (matching filters and adaptive subtraction) as a tool for removing multiples. If the image space subtraction is carried out on an ADCIG by ADCIG basis, the algorithm tries to account for the differences in amplitudes as well as the illumination range of modeled and recorded multiples. Adaptive matching works well for the ADCIGs corresponding to this example. When we do multiple removal in the data domain, we also use adaptive subtraction, but it is easier to match the missing parts in the angle domain, since the patterns are much simpler. If the velocity is perfect, events in the angle domain are flat. Secondly, in the angle domain we can enhance the performance of adaptive subtraction using the stack-and-spray approach or the Radon transforms in the case of complex situations, which is difficult to do when we are dealing with subtraction in the data domain.

In Figure 9, I compare angle gathers for the original multiple model, the reconstructed multiple model generated using a stack-and-spray approach, and the one reconstructed using the adaptive-matching algorithm. Once we reconstruct the missing angles, we can carry out the process of subtraction.

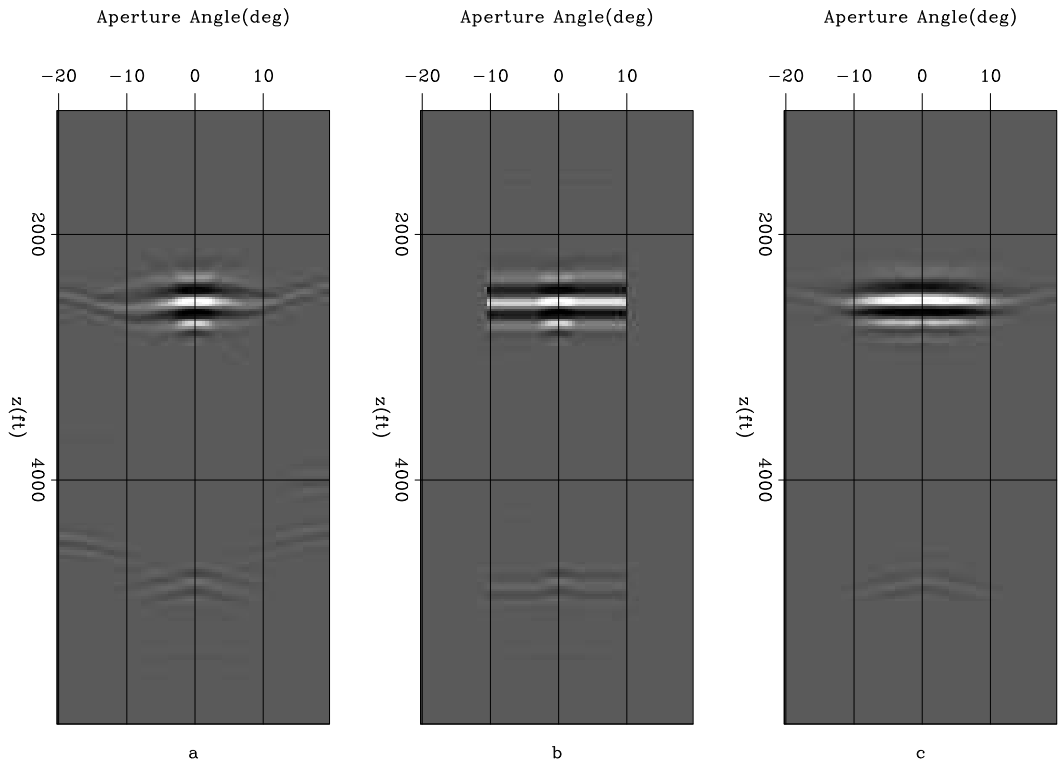

Figure 9: ADCIG for (a) multiple model and reconstructed multiple model using (b) stack and spray and (c) adaptive approach madhav1-recon [CR]

Finally, let us compare the image and the ADCIGs created by doing multiple removal in the data space to the one created in the image space using adaptive subtraction, working on one ADCIG at a time. Figure 10 is the result of multiple removal in the data space followed by migration, and Figure 11 is the result of multiple modeling in the image space followed by adaptive subtraction. The ADCIGs on right show the remains of the multiple energy in the former case at high angles, but nearly all the energy is gone in the latter.

SIGSBEE

Moving to a more realistic and complex subsurface geometry, in this section I discuss the application of SRMP on the Sigsbee data set. Figure 12 and 13 show the Sigsbee velocity model and the migrated image respectively. Figure 14 shows the corresponding multiple model in the image space. The side face in these figures is a representative ADCIG corresponding to sediments, left of the salt body. Since we migrate with the correct velocity, primaries appear flat in the ADCIGs, and multiples show a frown since they are migrated with velocities higher than their actual velocities.

The complex velocity model and especially the salt body cause the multiples to image in a very complicated fashion. It is difficult to identify even the water-bottom multiples that image underneath the salt body. Our goal here is to analyze multiples modeled by SRMP

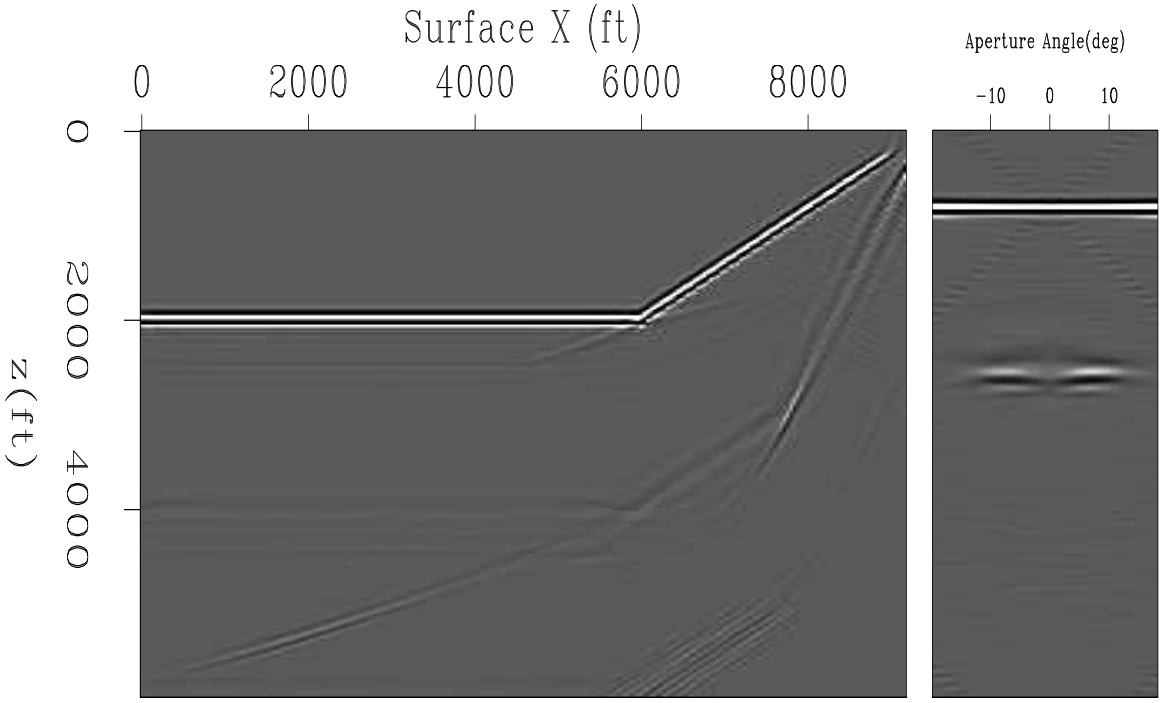

Figure 10: Image and a representative ADCIG at a surface location of 8000, created by data space multiple removal followed by migration madhav1-imgbf [CR]

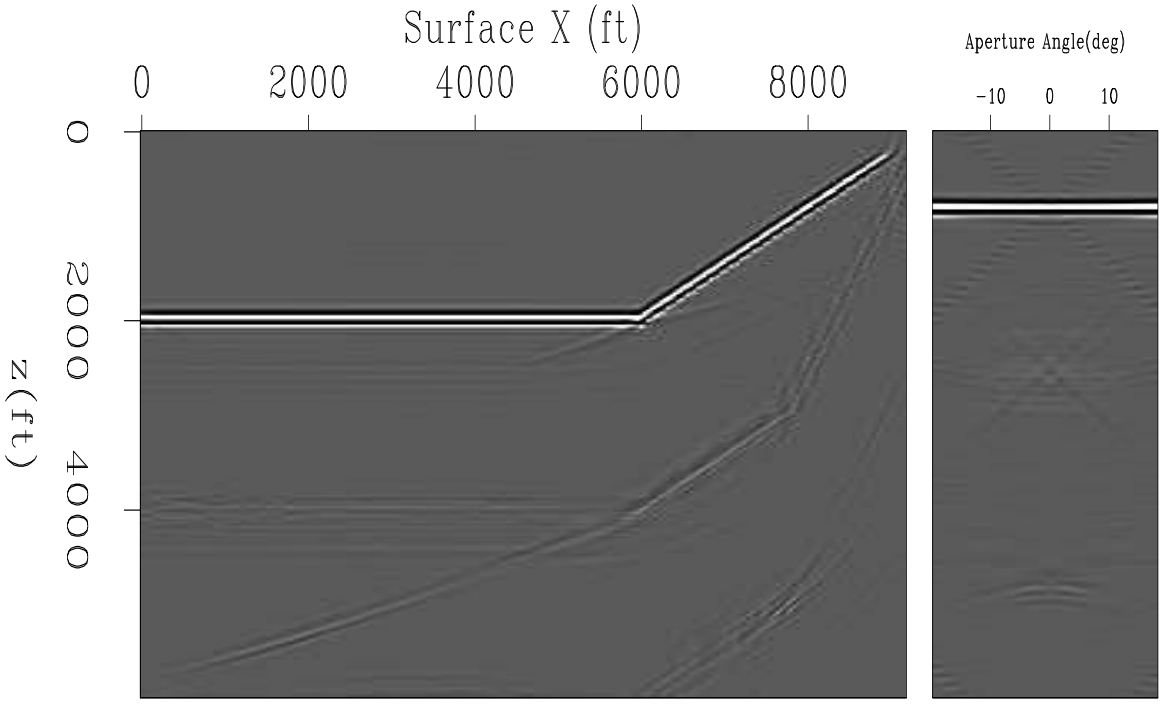

Figure 11: Image and a representative ADCIG at a surface location of 8000, created by image space multiple removal madhav1-imgaf [CR]

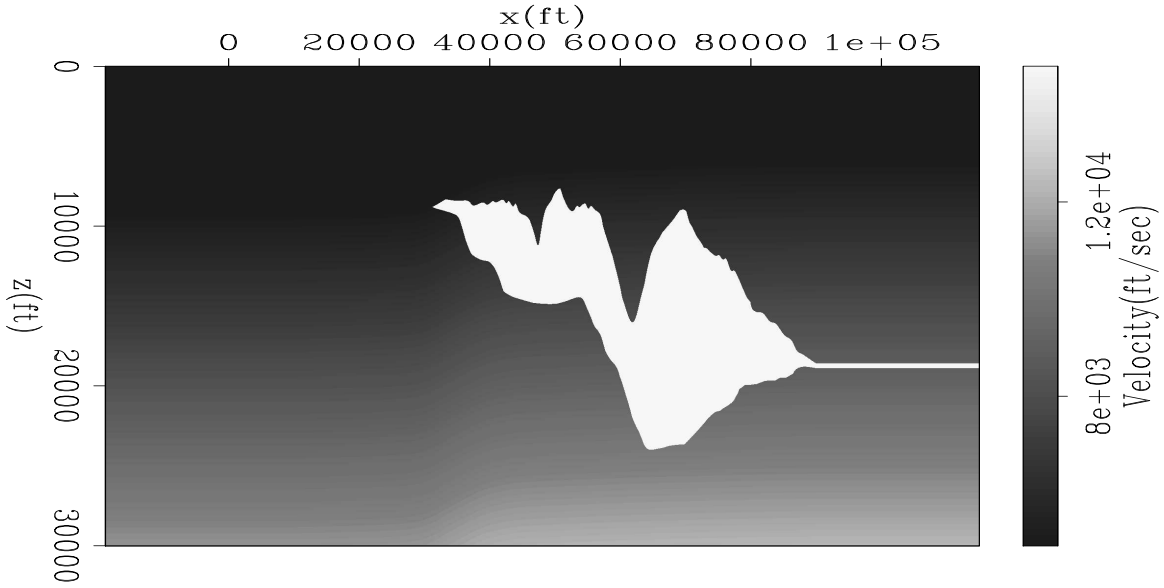

Figure 12: Velocity model for the Sigsbee data madhav1-vel.sig [NR]

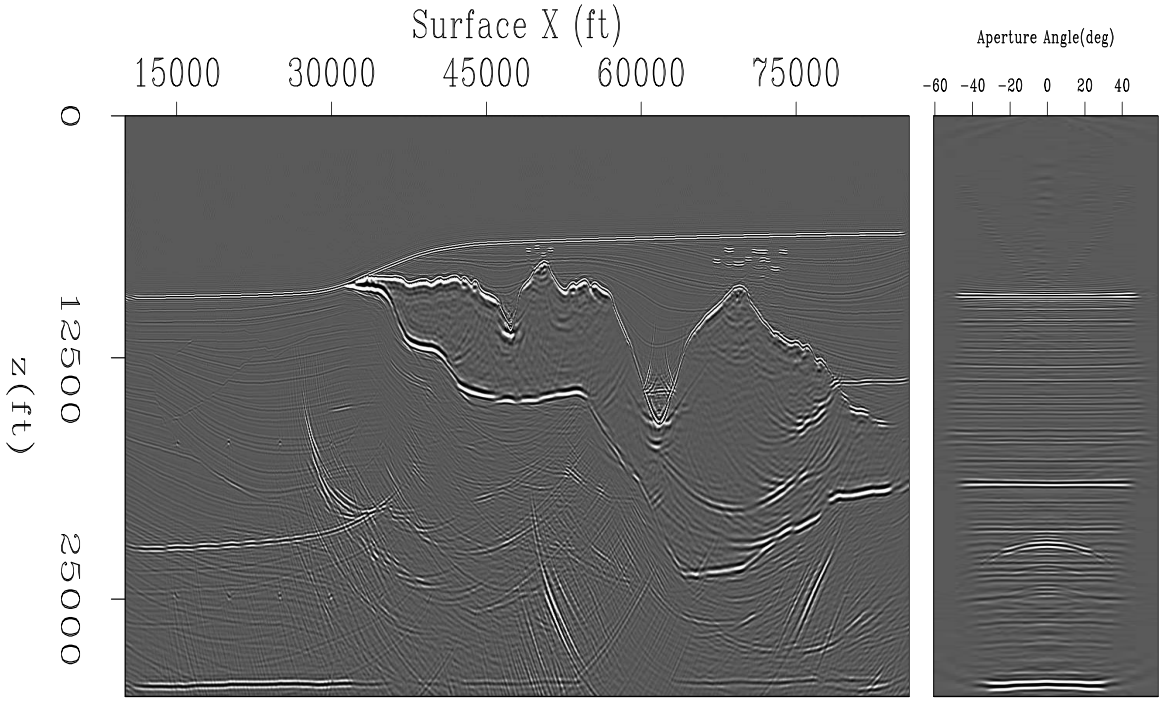

Figure 13: Image and a representative ADCIG for Sigsbee data migrated with the true velocity madhav1-imgtr.sig [CR]

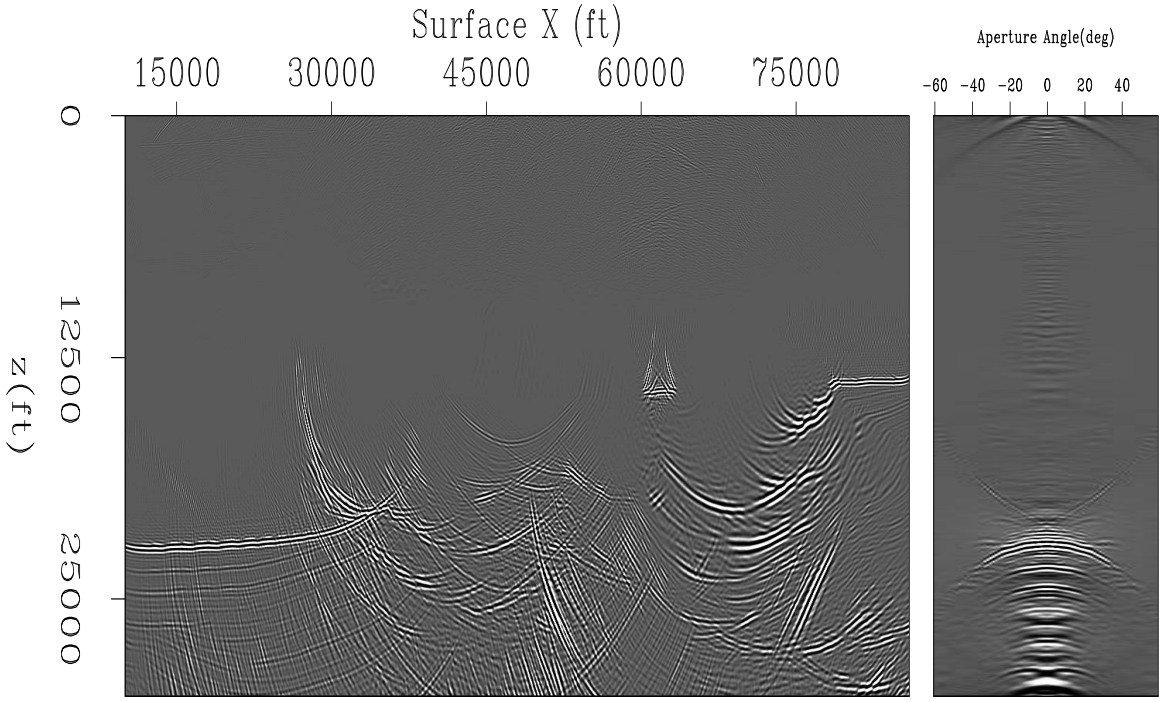

Figure 14: Multiple model (in image space) and a representative ADCIG for the Sigsbee data migrated with the true velocity madhav1-multr.sig [CR]

and improve our estimate if we have some missing parts in our model. Ideally, we would like to look at multiples in a domain where they can be easily identified and understood. To accomplish this I use water velocity as the migration velocity. Not all multiples travel at the water velocity, but many that emanate from shallow layers almost do that. Figures 15 and 16 show the image and the multiple model, with an ADCIG on the side. The first- and second-order water-bottom multiples look much more interpretable as we used water velocity for migration. These multiple events also appear flat in ADCIGs.

The Sigsbee data set has offsets of about 30000 ft. To illustrate the limitations of SRMP in the case of limited-offset recordings, I retain only near offsets (5000 ft) to model the multiples. In Figure 17, I compare the image (top) with the multiple model (bottom). Second-order multiples corresponding to the dipping part of the water bottom and salt canyon are present in the image but are not modeled using SRMP (compare circled events). These events correspond to the ray paths that tend to bounce back into the recording geometry, which we could not model because of limited recording offsets.

To demonstrate the possible use of angle gathers in SRMP, I focus on the dipping part of the first-order water-bottom multiple. The dip of that part is about 10°. Figure 18 (a) shows the ADCIG drawn from the image around the location of the dipping water bottom. Figure 18 (b) is the ADCIG of the multiple model at the same location. The first-order water-bottom multiple (at about a depth of 15000 ft) is illuminated at a much wider range of angles than it is actually modeled. If we subtract the multiples in the data space and then migrate the resulting

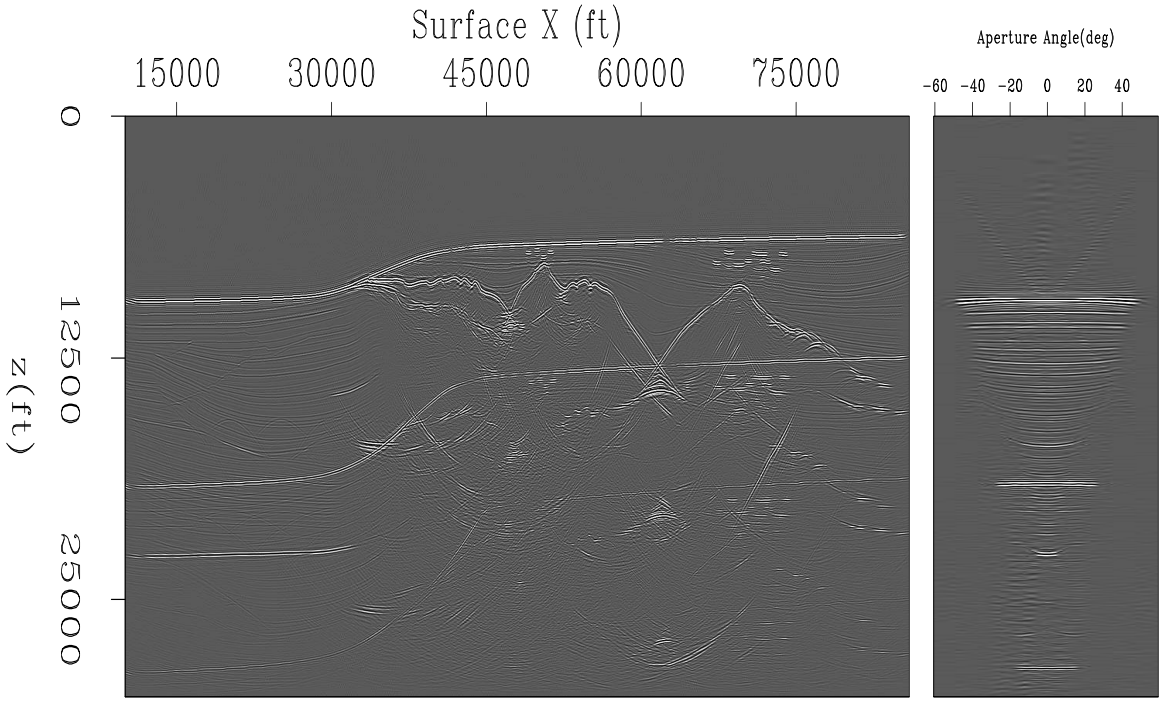

Figure 15: Image and a representative ADCIG for Sigsbee data migrated with the water velocity madhav1-imgwv.sig [CR]

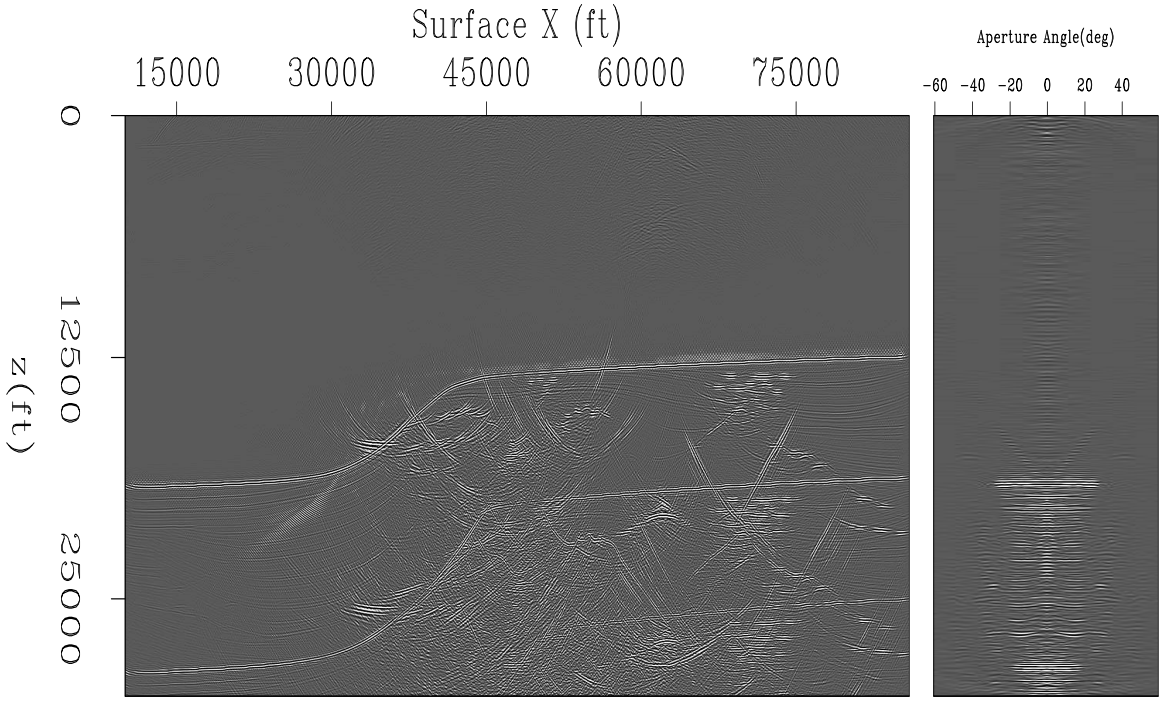

Figure 16: Multiple model (in image space) and a representative ADCIG for the Sigsbee data migrated with the water velocity madhav1-mulwv.sig [CR]

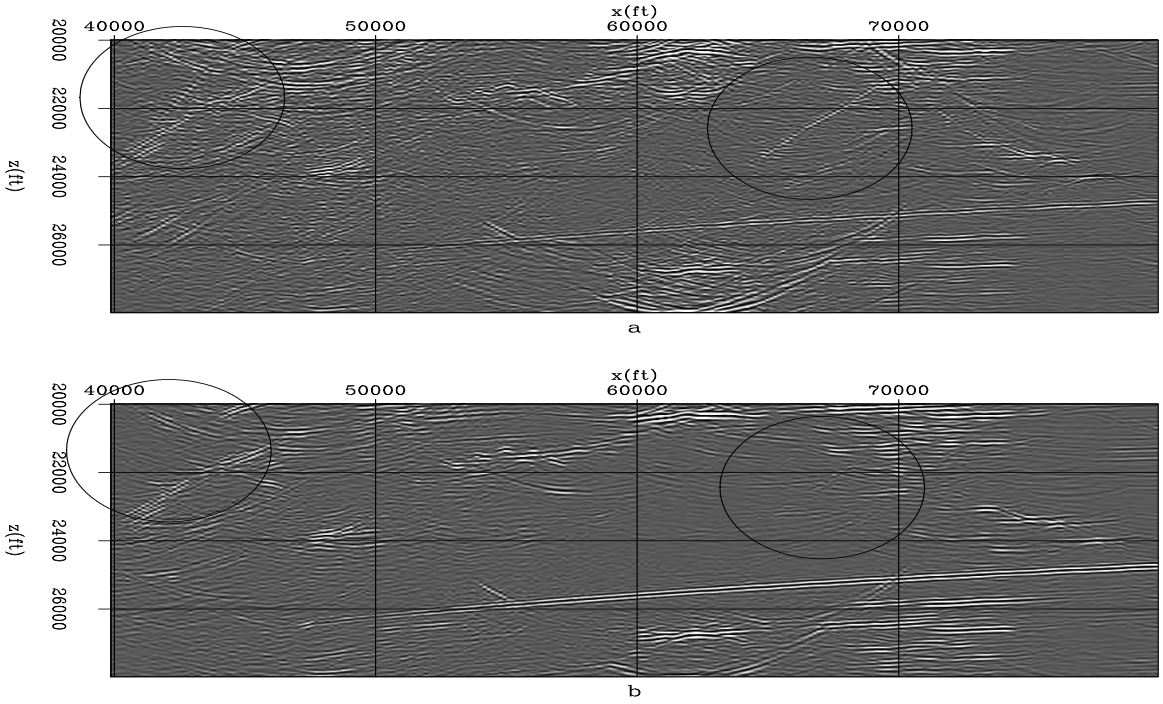

Figure 17: A window extracted from the (a) image and (b) the multiple model after migrating with the water velocity. madhav1-smloff.comp [CR]

data set, our image has some remnants of the multiple, which is understandable, since we did not model all the multiples that we recorded. Figure 18 (c) is the ADCIG from the same location, but corresponding to the data for which we subtract modeled multiples in the data space. For the specific water-bottom multiple, the energy is removed close to the zero opening angle but is present at higher opening angles. This observation is similar to the one in the simple synthetic example discussed in the previous section.

As in the simple synthetic example applying adaptive subtraction in the image domain gives us a better chance of removing this class of multiples. This is because in the angle space, multiples appear flat when migrated with the perfect velocity, and it is relatively straightforward for the matching filters to adaptively match the pattern of recorded multiples. When the velocity is not perfect, and multiples show curvature, it may be better to use Radon transforms to reconstruct missing multiples at higher opening angles. To draw a comparison for the given example, I plot in Figures 19 (a), (b) and (c) the ADCIG for the modeled multiple, the reconstructed multiple using the matching filter, and the multiple-free gather after subtraction in image space. The angle gather looks relatively cleaner after subtraction in the image domain (right panel).

Since we carried out migration with the water velocity, we now demigrate with the water velocity and re-migrate with the true velocity to obtain a multiple-free image. This proposition appears expensive, but may be useful when the multiple noise is overwhelming. Again, an alternative may be to use the true velocity but use Radon transforms to infill missing angles

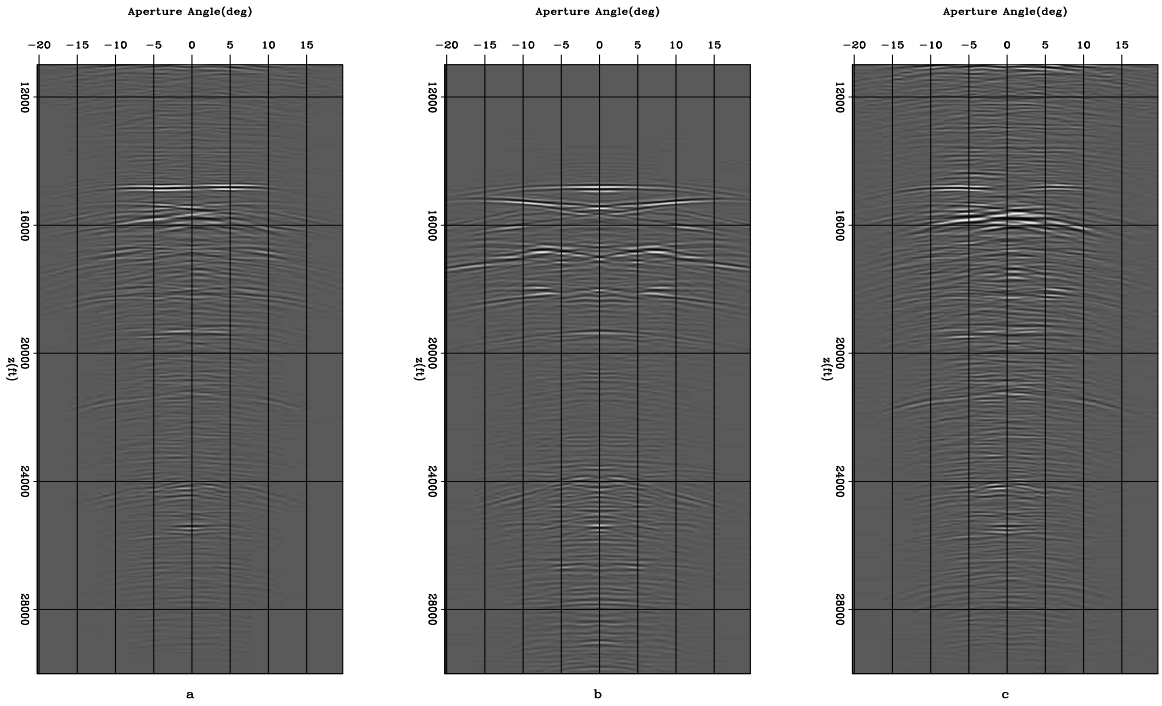

Figure 18: ADCIG for (a)the image, (b) the multiple model and (c) the image after multiple removal in the data domain madhav1-adcig.sig [CR]

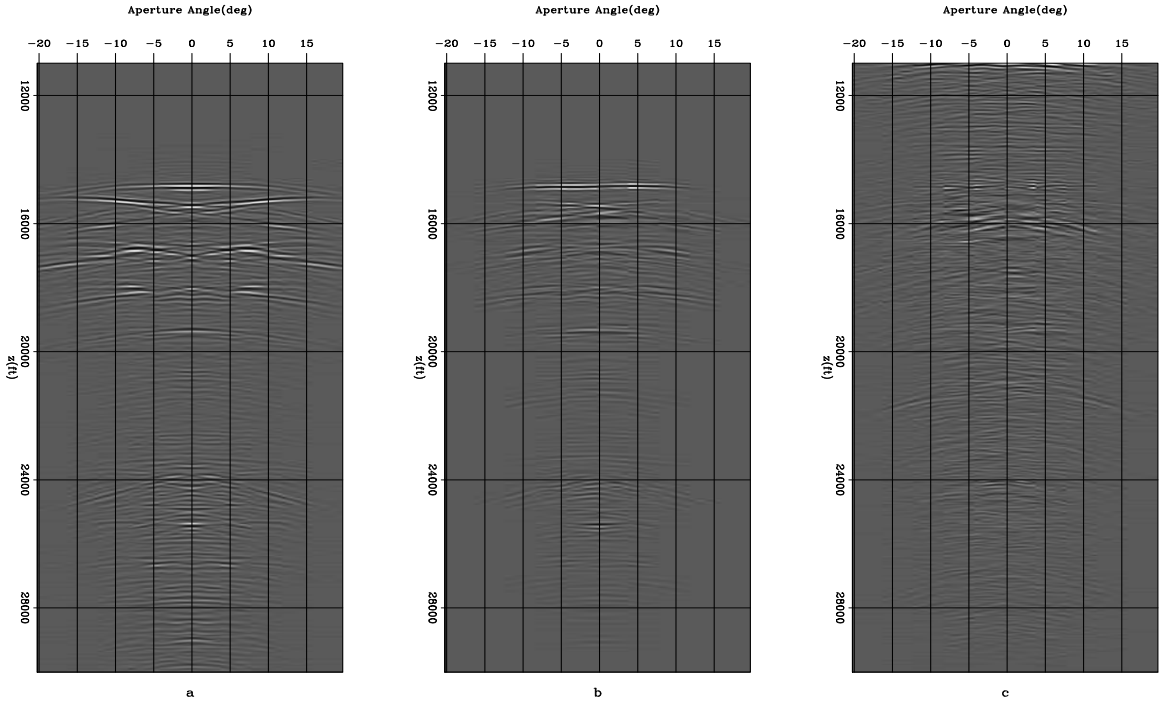

Figure 19: ADCIG for (a) the multiple model, (b) the reconstructed multiple model and (c) the image after multiple removal in image domain madhav1-adcig2.sig [CR]

and assist adaptive subtraction in the angle domain.

DISCUSSION AND CONCLUSIONS

Surface-related multiple prediction works well for predicting the free-surface multiples, but, as shown through a series of tests and examples, it fails for certain ray paths where the subsurface geometry is complicated, and we have access to only small offsets. Though data-space and image-space SRMP are mathematically equivalent, image-space subtraction gives us a better chance of reconstructing the missing parts of the multiple model because of the redundancy associated with the image space. In the present analysis we used angle gathers as a preferred domain of reconstruction.

In the presence of complicated structures and salt bodies, multiples migrate to the image space in a fairly complicated fashion when we use the true migration velocity. The use of the multiple velocity for migration takes us to a domain where multiples are identifiable and appear flat in ADCIGs. We may carry out the process of reconstruction relatively easily in this domain. But the drawback is that this should be followed by the process of demigration and migration, making it computationally very expensive. As discussed earlier, we may also use Radon-style transforms for reconstruction, which should work even when the multiples are not absolutely flat in ADCIGs. This allows us to migrate with the true velocity in one step, avoiding the extra steps of migration and demigration. Although the performance of the Radon transform depends upon how many angles we actually have, in the case of a very narrow range of angles, the spectrum would be very smeared, and effective reconstruction would not be possible.

To illustrate these points, in the examples above I retain only very small offsets, which might appear unrealistic for the inline direction. However, there is a trade-off between the offsets and dip of the structure; for instance, if dip is very high, SRMP can fail even for large recording offsets. Furthermore, in 3D surveys, along with many limitations of SRMP, extremely limited crossline offsets might be a concern for even a gently dipping water bottom. The heuristic extension of the idea discussed here would be that in 3D, a multiple event might be perfectly modeled for some azimuths, but not all. In that case we may spread information across azimuths to reconstruct the multiple model, like we did across aperture angles in the 2D case.

ACKNOWLEDGMENTS

The author would like to thank the SMAART JV for the Sigsbee dataset. I would like to thank Biondo Biondi for his guidance and suggestions through out this work. Also I would like to thank Bob Clapp and Gabriel Alvarez for very useful and insightful discussions that helped shape the project.

REFERENCES

Alvarez, G. and A. Guitton, 2006, Simultaneous adaptive matching of primaries and multiples with non-stationary filters: SEP, **125**, 61–75.

Alvarez, G., B. Biondi, and A. Guitton, 2004, Attenuation of diffracted multiples in angle-domain common-image gathers: 74th Annual International Meeting, SEG, Expanded Abstracts, 1301–1304.

Anstey, N. A. and P. Newman, 1966, The sectional auto-correlogram and the sectional retro-correlogram: Geophysical Prospecting, **14, No.4**, 389–426.

Artman, B. and K. Matson, 2006, Image-space surface-related multiple prediction: SEP, **125**, 47–60.

Berkhout, A. J. and D. J. Verschuur, 1997, Estimation of multiple scattering by iterative inversion, part i:theoretical considerations: Geophysics, **62**, no. 5, 1586–1595.

Sava, P. and A. Guitton, 2003, Multiple attenuation in the image space: 73rd Annual International Meeting, SEG, Expanded Abstracts, 1933–1936.

Sava, P. and A. Guitton, 2005, Multiple attenuation in the image space: Geophysics, **70**, 10–20.